

## RESEARCH ARTICLE

# Enhanced Multi-Synchro-Squeezing Transform for Fault Diagnosis in Induction Machine Based on Third-Order Energy Operator of Stator Current Signature

REZA BAZGHANDI<sup>1</sup>, MOHAMMAD HOSEINTABAR MARZEBALI<sup>1</sup>,  
AND VAHID ABOLGHASEMI<sup>2</sup>, (Senior Member, IEEE)

<sup>1</sup>Faculty of Electrical Engineering, Shahrood University of Technology, Shahrood 36199-95161, Iran

<sup>2</sup>School of Computer Science and Electronic Engineering, University of Essex, CO4 3SQ Colchester, U.K.

Corresponding authors: Mohammad Hoseintabar Marzebali (m.hoseintabar@shahroodut.ac.ir) and Vahid Abolghasemi (v.abolghasemi@essex.ac.uk)

**ABSTRACT** In traditional motor current signature analysis (MCSA) approach, the spectral leakage of the fundamental supply frequency can obscure the characteristic fault component under low-load or no-load conditions. Furthermore, most time-frequency (TF) methods often have low resolution and are not qualified to produce a narrow band in the output. In this paper, we employ multi-synchro-squeezing transform (MSST) to show its effectiveness in fault detection of induction machines, for the first time. The key innovation of this work is merging MSST (due to its high time-frequency resolution) with the third-order energy operator (TOEO) (due to its high accuracy in fault detection). Specifically, TOEO is used to overcome the leakage effects of the supply frequency, through a demodulation approach for asymmetric fault detection along with MSST technique. The proposed method was evaluated for induction machine fault detection in both steady-state and transient conditions. Both analytical and experimental results confirm that the proposed method can excellently reveal the fault characteristic frequency in steady-state and transient mode, instead of the sideband frequencies.

**INDEX TERMS** Fault diagnosis, condition monitoring, induction machine, fast Fourier transform, current signature.

## I. INTRODUCTION

Condition monitoring for industrial tools is crucial as it enables proactive maintenance, preventing unexpected breakdowns and minimizing downtime. By continuously assessing the health and performance of equipment, organizations can optimize operational efficiency, extend the lifespan of tools, and ultimately reduce overall maintenance costs [1], [2]. Among these, induction machines (IMs) are crucially important due to their use in various industrial applications [3], [4]. Due to inappropriate operational and environmental conditions and unexpected events, many IMs have failed, leading

to heavy financial losses. Therefore, condition monitoring is necessary and unavoidable [5]. In this regard, IMs face different mechanical and electrical faults. In general, these failures mainly cause asymmetry in the rotor circuit of machine [6]. If the mentioned faults and failures are not detected, the machine will suffer from many problems such as high thermal stress, a winding fault, broken rotor bars (BRBs), misaligned rotor, etc. [7], [8]. Consequently, timely and prompt detection of faults occurred in the machine is essential to ensure IMs' safety and operational efficiency.

Various diagnostic techniques were reported in the past to ensure the optimal performance of the induction machines and guarantee the safety of IMs such as motor current signature analysis (MCSA) [9], [10], vibration analysis [11],

The associate editor coordinating the review of this manuscript and approving it for publication was Sinisa Djurovic.

[12], stray flux signals [12], [13], deep learning [14], and acoustic emission analysis [15]. Among mentioned strategies, the MCSA method has attracted more attentions due to simplicity, non-invasive nature and cost-effectiveness. Despite all the advantages of MCSA, the classical MCSA is analysed by fast Fourier transform (FFT), which is still prone to several limitations in various real-world engineering and industrial applications. For example, in large IMs operating with very low slip or no-load conditions, the side-band frequencies (fault characteristic frequency) show a very low-energy component being too close to the fundamental frequency. This will significantly reduce the detection accuracy. Furthermore, traditional methods for examining time-frequency relationships, such as the short-time Fourier transform (STFT) and wavelet transform (WT) [16], [17], can convert a one-dimensional time series signal into a two-dimensional time-frequency plane. Unfortunately, the limitations of traditional time-frequency techniques significantly hinder their practical effectiveness.

To overcome the disadvantages of conventional methods and achieve a satisfactory time-frequency analysis, various approaches such as the time-reassigned synchro-squeezing wavelet transform (SSWT) [18], synchro-squeezing transform (SST) [19], [20], demodulated SST (DSST) [21], [22], high-order SST [23], [24] and Stockwell transform (S-Transform) [25] have been presented, previously. Recently, the multi-synchro-squeezing Transform technique (MSST) [26] was proposed for time-frequency (TF) analysis with high resolution capability of different time-varying signals in different applications. MSST has shown a breakthrough in time-frequency analysis by providing a high-contrast spectrum with distinguishable patterns. The significance of this approach is in detecting low-energy and overlapped components such as those occurring in faulty IMs. However, frequency leakage is still a problem in MSST which may generate blurry and inaccurate TF plane. The proposed method in this paper resolves these issues.

The reassignment method (RM) has been designed to improve the clarity of the initial time-frequency (TF) representation [27]. The key step in RM involves computing updated positions for each TF point using TF phase information. Subsequently, two-dimensional reassignment operations, focusing on both frequency and time reassignment, are utilised to consolidate the TF spectrogram along the TF axis. One drawback of RM is its incapacity to reconstruct the signal, a limitation inherent in the RM framework. SST strategy is another recent technique to achieve ideal TF analysis. Unlike the RM method, the SST method increases the TF resolution and enables signal reconstruction. Some recent studies show that SST cannot produce appropriate TF results when for time-varying signals [18], [22]. A higher-order SST has been proposed by the authors to achieve more accurate TF results while preserving the reversibility [28]. Regardless, by increasing the SST order, the computational cost also increases.

Third order energy operator (TOEO) is one of the energy operators that can perform demodulation operations well with low computational cost. Our idea is to use the MSST method along with TOEO, enabling us to create a high-resolution map in the output. Consequently, a high accuracy diagnosis can be obtained with a low computational cost. The presented method here reduces the spectral leakage and increases the resolution in the time-frequency analysis output, simultaneously. We evaluate the proposed method for asymmetric fault detection in a wound rotor induction machine (WRIM) operating in both steady-state and transient modes. To the best of the authors' knowledge, it is the first time where this combination is proposed for diagnosis of the asymmetric faults.

Although the MSST technique has been already presented for time-frequency analysis, no work is reported on the mechanical fault diagnosis of the induction motor using this method. To enhance the fault detection and separation, here, the MSST technique is combined with the TOEO as a demodulation method. The proposed method has been tested on two WRIM and SCIM motor with asymmetric and BRB faults. It has been found out that the combined MSST and TOEO technique clearly show the condition of machine in healthy and faulty conditions in the presence of faults. The key contributions of this study are summarised as follows:

- We introduce an advanced approach through merging MSST with TOEO to simultaneously take advantage of “high time-frequency resolution” and “high detection accuracy in fault detection”.
- Specifically, the incorporation of TOEO aids in overcoming the leakage effects of the supply frequency through a demodulation approach. To the best of our knowledge, this study represents the first to propose a modified MSST approach, combined with TOEO, for asymmetric fault diagnosis of induction motors.
- A series of synthetic and real experiments have been conducted to validate the performance of the proposed approach.

The organisation of this paper is as follows: in Section II, the fundamental theory of TOEO for current signature analysis is introduced. Then, the application of TOEO for asymmetric fault detection is described. In Section III, the theory of MSST strategy is described in detail. In Sections IV and V, analytical and experimental results have been investigated, respectively. In Section VI, a comparison between the proposed method and other approaches is provided. Finally, the conclusion is presented in Section VII.

## II. THIRD-ORDER ENERGY OPERATOR OF CURRENT SIGNATURE

This section discusses the introduction and mathematical definition of the higher order energy operators. After introducing the TOEO, its application is developed for the healthy and faulty stator current in IM. Higher order differential energy operators for a continuous-time signal

$y(t)$  are defined as follows [29]:

$$H_i(y) = [y, y^{(i-1)}] = y'y^{(i-1)} - yy^{(i)}, \quad i = 0, \pm 1, \pm 2, \pm 3, \dots \quad (1)$$

where  $y'(t)$  is the first-order derivative of the  $y(t)$ ,  $[\cdot]$  is the Lee bracket,  $x^{(i)}$ , indicating the derivative operation if  $i$  is positive and integral if it is negative.

$$y_i(t) = \begin{cases} d^i y(t)/dt^i & i \geq 1 \\ y(t) & i = 0 \\ \int_{-\infty}^t y^{(i+1)}(\tau) d\tau & i \leq -1 \end{cases} \quad (2)$$

where  $i$  is usually taken as a positive integer in most practical applications. If  $i = 2$  in (1), the same Teager-Kaiser Energy Operator (TKEO) equation is obtained. However, considering  $i = 3$ , then  $H_3[y(t)]$ , the equation of the TOEO is obtained, which is a speed energy operator. Energy operators of higher orders, such as third or fourth-order operators, have the ability to emphasise energy and impact components more effectively. However, employing higher-order energy operators significantly escalates computational complexity. Consequently, taking all constraints into account, this paper opts for the third-order energy operator (TOEO,  $i = 3$ ). The TOEO for a signal  $y(t)$  can be mathematically expressed as follows:

$$H_3(y) = y'(t)y''(t) - y(t)y'''(t) \quad (3)$$

Due to having discrete signals in practical work, (3) cannot be used to calculate TOEO. Therefore, (3) should be rewritten in discrete form. Replacing the continuous signal  $y(t)$  with the discrete signal  $y[n]$ , sampled with the sampling sequence  $n\Delta t$ , leads to (5). We can now calculate the signal  $y(t)$  derivatives with the backward difference operator:

$$y'(t) = \frac{y[n] - y[n-1]}{\Delta t} \quad (4)$$

$$H_3\{y[n]\} = y[n]y[n+1] - y[n-1]y[n+2] \quad (5)$$

where  $1/\Delta t$  is the sampling frequency. As seen in (5), only two multiplications and one addition are required to calculate the TOEO approach. This can noticeably reduce the computational burden. Compared to other methods such as normalized frequency domain energy operator (NFDEO) [30] or sum of adjacent products SAP [31], the TOEO can more effectively highlight the asymmetric fault index with some simple calculations.

The stator current equation for a normal motor fed by a sinusoidal power supply can be written as follows [30]:

$$i_H(t) = I_m \cos(\omega_s t) = I_m \cos(2\pi f_s t) \quad (6)$$

where  $\omega_s$  is the angular frequency and is equal to  $2\pi f_s$ ,  $f_s$  is the supply frequency (50/60Hz) and  $I_m$  is the maximum stator current. In induction motors with faults such as BRB or internal short circuits in the rotor windings of WRIM, periodic disturbances caused by the faults result in amplitude

and phase modulation of the stator current at the characteristic fault frequency ( $f_f = 2sf_s$ ). When solely taking amplitude modulation into account, the expression for the stator current signature of a faulty motor is as follows:

$$\begin{aligned} i_F(t) &= i_H(t)[1 + \beta \cos(2\pi f_f t)] \\ &= I_m \cos(2\pi f_s t) + \frac{I_m \beta}{2} \cos(2\pi(f_s + f_f)t) \\ &\quad + \frac{I_m \beta}{2} \cos(2\pi(f_s - f_f)t) \end{aligned} \quad (7)$$

where  $\beta$  is the asymmetric fault modulation index and  $s$  is the motor slip. Generally,  $\beta \ll 1$ , therefore, the amplitudes of the sidebands corresponding to the fault,  $f_s \pm f_f$ , is much smaller than the amplitude of supply frequency ( $f_s$ ). By merging (4) and (7), we can obtain the stator current signal in faulty IM as follows [32]:

$$\begin{aligned} i_{TOEO,F}(t) &= -\frac{I_m^2 \beta \omega_F}{2} (4\omega_s^2 + \omega_F^2) \sin(\omega_F t) \\ &\quad - I_m^2 \beta^2 \omega_s \omega_F (\omega_s \sin(2\omega_F t) + \omega_F \sin(2\omega_s t)) \\ &\quad - \frac{I_m^2 \beta \omega_F^2}{4} (\omega_F + 2\omega_s) \sin((\omega_F + 2\omega_s)t) \\ &\quad - \frac{I_m^2 \beta \omega_F^2}{4} (\omega_F - 2\omega_s) \sin((\omega_F - 2\omega_s)t) \end{aligned} \quad (8)$$

The demodulated current signal from TOEO eliminates the fundamental component. Therefore, the spectral leakage because of the fundamental supply frequency will be eliminated. As can be seen, it is much easier to detect the fault index in the TOEO current spectrum ( $i_{TOEO,F}(t)$ ) than in stator current spectrum ( $i_F(t)$ ). It should be noted that TOEO is zero for a healthy IM. Consequently, the demodulated current by TOEO for a faulty IM does not include the DC component. Therefore, there is no necessity to eliminate the constant term in (8). This distinction sets the TOEO method apart from other established demodulation techniques like TKEO and rectification [33], [34]. Figure 1 depicts the flowchart of different steps of the proposed method in this study.

### III. MULTI-SYNCHRO-SQUEEZING TRANSFORM

Recently, several time-frequency (TF) techniques have been introduced, but many of these methods offer limited frequency resolution and are unable to produce a narrow band in their output response. Linear time-frequency approaches entail computing the inner product of the signal and the basis function, aiding in the detection of local, time-varying features. In accordance with inner product theory, a basis function that aligns effectively with the non-stationary signal can provide a more precise description of its concentrated energy time-frequency characteristics [35]. Consequently, to handle signals undergoing significant time-related changes, non-linear TF methods have emerged. These methods achieve this by demodulating the frequency-modulated (FM) component [36].

In practical applications, non-parametric and non-demodulated Synchrosqueezing Transform (SST) is often

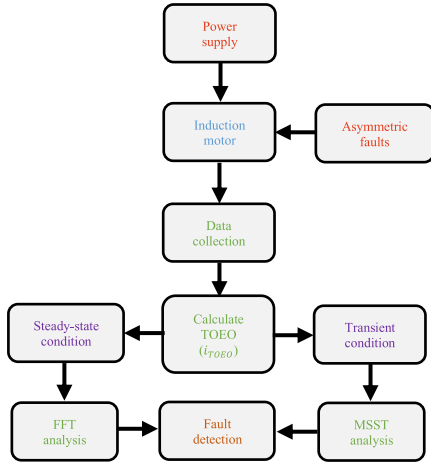


FIGURE 1. Flowchart of the proposed method.

very practical. A second-order SST, introduced in [37], has been designed to offer a high-resolution time-frequency (TF) representation while maintaining reversibility. In 2017, a higher-order SST was proposed to achieve more focused TF results [23]. However, higher SST orders also lead to increased computational complexity. For instance, the first-order SST (primary SST) requires only one STFT operation, whereas the fourth-order SST necessitates eleven STFT operations. Generally, the Modified Synchrosqueezing Transform method offers an iterative approach with lower computational complexity compared to high-order SST, effectively enhancing energy concentration in dealing with highly time-varying signals. To obtain the MSST output response, the STFT operation is executed only once, which causes a low computational cost in performing this method. First, we show the time-varying single-component signal as follows:

$$x(t) = A(t)e^{j\phi(t)} \quad (9)$$

where  $A(t)$  is the maximum amplitude of the signal and  $\phi(t)$  shows the phase of the signal. Now, the STFT of the above signal can be written as follows:

$$S(t, \omega) = \int_{-\infty}^{+\infty} w(u-t)x(u)e^{-j\omega(u-t)} du \quad (10)$$

where  $w(u)$  is the window function.  $x(t)$  is considered as the pure and clean signal within a short period of time. With this assumption and according to the Taylor expansion equation (11) can be written as:

$$\begin{aligned} A(u) &= A(t) \\ \phi(u) &= \phi(t) + \phi'(t)(u-t) \end{aligned} \quad (11)$$

The first order Taylor expansion is shown in (11) where  $\phi'(t)$  is derivative of  $\phi(t)$ . As a result,  $x(t)$  can be expressed as follows.

$$x(u) = A(u)e^{j(\phi(t) + \phi'(t)(u-t))} \quad (12)$$

Finally, by means of STFT  $x(t)$  can be converted into the following form by (10):

$$\begin{aligned} S(t, \omega) &= \int_{-\infty}^{+\infty} w(u-t)A(t)e^{j(\phi(t) + \phi'(t)(u-t))} e^{-j\omega(u-t)} du, \\ &= A(u)e^{j\phi(t)} \int_{-\infty}^{+\infty} w(u-t)e^{j(\phi'(t)(u-t) - j\omega(u-t))} d(u-t), \\ &= A(u)e^{j\phi(t)} \hat{w}(\omega - \phi'(t)), \end{aligned} \quad (13)$$

where  $\hat{w}$  is the Fourier transform of  $w$  and  $t$  and are time and frequency, respectively. After calculating the derivative of  $S(t, \omega)$  with respect to time, we have:

$$\begin{aligned} \partial_t S(t, \omega) &= \partial_t \left( A(u)e^{j\phi(t)} \hat{w}(\omega - \phi'(t)) \right) \\ &= A(u)e^{j\phi(t)} \hat{w}(\omega - \phi'(t)) j\phi'(t) \\ &= S(t, \omega) j\phi'(t) \end{aligned} \quad (14)$$

SST equation ( $T_s(t, \psi)$ ) is described as follows [16]:

$$T_s(t, \psi) = \int_{-\infty}^{+\infty} S(t, \omega) \delta(\psi - \hat{\omega}(t, \omega)) d\omega \quad (15)$$

Finally, the MSST equation can be obtained by iteration of the SST method.

$$T_s^{[i]}(t, \psi) = \int_{-\infty}^{+\infty} T_s^{[i-1]}(t, \omega) S(t, \omega) \delta(\psi - \hat{\omega}^{[i-1]}(t, \omega)) d\omega \quad (16)$$

where  $i$  is the number of iterations. Finally, the corresponding instantaneous frequency estimate obtained from MSST is calculated as follows:

$$\hat{\omega}^{[i]}(t, \psi) = \phi'(t) + \left( \frac{\phi''(t)^2}{1 + \phi''(t)^2} \right)^i (\psi - \phi'(t)) \quad (17)$$

With multiple iterations (17), a new frequency is estimated, which is closer to the accurate instantaneous frequency through redistributing sparse STFT coefficients [26].

#### IV. ANALYTICAL RESULTS

The TOEO method is first applied to the analytical signals to start the fault diagnosis, and the TOEO current is obtained. When obtaining the fault current, by considering the conditions of the analytical signal (transient and steady-state mode), fast Fourier transform or MSST methods can be implemented on the demodulated signal.

The presented technique has been investigated through synthetic signal of stator current of IM in MATLAB software environment. To describe the validity of the presented approach here, the synthetic signal of stator current with simplified combination of fault-related frequency and supply frequency introduced in (6) with the parameters given in Table 1 is considered. The synthetic current signal has been analysed in two modes: 1) steady-state and 2) transient

TABLE 1. Specification of analytical signal.

Parameter	Value
$I_m(A)$	1
$f_s$	50
$\beta$	0.1
$s$	0.02
$f_F(Hz)$	2

mode. The parameters of the processed signal are specified in Table 1. The slip in the steady state is assumed to be 0.02, and small slip changes have been applied in transient mode, which is initially 0.02 and finally reaches 0.03. The slip changes are applied to the synthetic signal in the sixth second in transient condition. In order to have a high resolution in synthetic signal, a sampling frequency of 10 kHz is considered.

A. STEADY-STATE CONDITION

Fig. 2a illustrates the synthetic signal with a sampling frequency of 10 kHz and a duration of 12 seconds used for verifying the presented method. The rotor asymmetry fault is simulated as sideband frequencies around the fundamental frequency. In the Fourier transform of the main signal, the fundamental frequency has the highest amplitude (50Hz), and the severity of the side frequencies is lower than the main component (Fig. 2b). The demodulated signal by the TOEO technique can be observed well in Fig. 2c. As mentioned, the slip equals 0.02, and the FFT of the TOEO signal shows the fault characteristic frequency (Fig. 2d).

B. TRANSIENT CONDITION

In this part, the presented method in transient mode is validated. The synthetic signal introduced in (7) has been analysed in this section. In order to simulate the arbitrary variation in the synthetic signal, the slip has two different values. In this regard, the synthetic signal is divided into two parts from 0 to 6 seconds and 6 to 12 seconds. In the first step, the slip equals 0.02, and finally the slip reaches 0.03.

In our study, the MSST technique is adapted for fault detection under the transient mode, which is illustrated in Fig. 3b and d. As can be seen from Fig. 3b and d, the MSST approach has a very high resolution and creates a narrow band in its output response. In the MSST of the analytical signal, the fundamental frequency component has the highest severity, and asymmetric fault is undetected in this signal. After demodulating the analytical signal and obtaining the TOEO signal, MSST can be used to detect the asymmetric fault in the transient mode.

V. EXPERIMENTAL RESULTS

In this section, we initially detail the process of acquiring stator current data from the Wound Rotor Induction Motor as part of evaluating the effectiveness of the proposed method. Subsequently, the stator current signals obtained from the

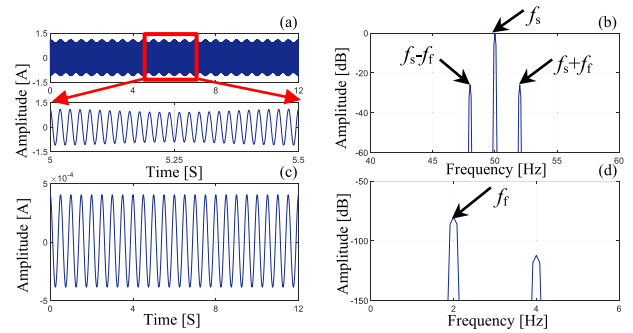


FIGURE 2. Steady-state conditions with synthetic signals (sampling frequency of 10 kHz for at  $s = 0.02$ ): stator current waveform under fault conditions during spectral analysis of the proposed method in a) time and b) frequency domains. The demodulated signal (TOEO) corresponding to the asymmetry fault in c) time and d) frequency domains.

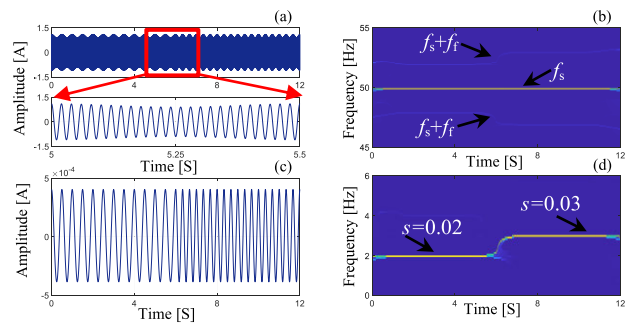
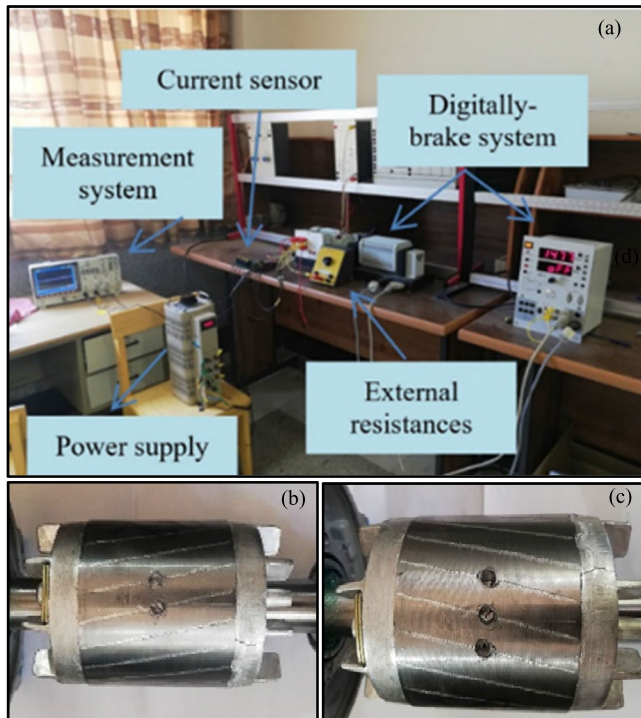


FIGURE 3. a) Synthetic signal of stator current in transient conditions with presence of an asymmetry fault. b) MSST analysis for the stator current signature in transient mode. c) Demodulated signal corresponding to the asymmetry fault. d) MSST analysis for the TOEO signal.

experimental platform are employed to assess the proposed strategy for detecting asymmetric faults in both steady-state and transient conditions. Ultimately, the performance and effectiveness of the TOEO strategy are evaluated in conjunction with the MSST technique.

A. TEST-RIG DESCRIPTION

We applied our method to a Wound Rotor Induction Machine to assess its effectiveness. In this test, there are two types of faults for two different machines. First, the asymmetric fault (high resistance connection) for the wound rotor machine and second the BRB fault for the SCIM was tested. Since these two faults have specific fault index ( $2sf_s$ ) in the current signature of machine, both machines are considered in this paper to show the variation of fault in different fault severity in the presence of rotor asymmetric fault. These tests were conducted under both steady-state and transient conditions. The transient conditions were further categorised into two states: acceleration and deceleration. In Squirrel Cage Induction Machines (SCIM), Broken Rotor Bars (BRBs) result in an asymmetric fault in the machine’s rotor circuit. Conversely, in WRIM, the asymmetric fault arises when the rotor coils experience a short circuit over a period of time. However, to model an asymmetric fault in WRIM, an external resistance



**FIGURE 4.** Test-rig system description of WRIM and SCIM used for asymmetric fault detection -b) Two BRBs -d) Three BRBs.

to one of the rotor winding phases is applied and then the stator current data of single phase is collected through current sensors (Fig.2a). In this experiment, a Hall Effect Current Sensor (S25P100D15X), as depicted in Fig.2b, was employed to measure the current. The experimental results are collected through test-rig presented in Fig.2a. The tests have been performed for SCIM with BRBs (Fig.2c and Fig.2d) and WRIM with external resistance in the circuit of rotor windings.

The signals extracted in steady-state condition have a sampling frequency of 2kHz and have a length of 25k. For the transient mode, the sampling frequency has increased to 2.5kHz, and the signal length has risen to 32k. The speed of the machine is constant and equal to 1470 RPM for steady-state condition. In transient condition, the motor speed changes from 1400 to 1450 RPM, and 1450 to 1400 RPM for acceleration and deceleration condition, respectively.

Fig. 4 shows the test-rig used for fault detection test in this paper. As can be observed, current sensors and measuring device are used to record and collect data, external resistance is used to model asymmetric fault in WRIM. The external resistance applied to create for an asymmetric fault is 0.14p.u, which is equal to the severity of the asymmetric fault. Since the external resistance in the rotor winding varies extensively, in this paper the rotor asymmetry is modelled as external resistance in the rotor winding of WRIM. A digital brake system has been used to control the speed or torque of WRIM. More parameters of WRIM are presented in Table 2.

**TABLE 2.** Specification of WRIM.

Parameters	Value
Rated voltage ( $V$ )	380
Rated power ( $W$ )	270
Supply frequency ( $Hz$ )	50
Pole pairs	2
Stator winding connections	Y
Stator winding resistance ( $\Omega$ )	34.73
Rotor winding resistance ( $\Omega$ )	32.12
Mutual inductance ( $H$ )	1.339
Self-inductance of stator ( $H$ )	0.139
Self-inductance of rotor ( $H$ )	0.159
Inertia ( $kg.m^2$ )	0.00161

### B. STEADY-STATE CONDITION

First, we will examine the results of a healthy type of motor that works at a speed of 1500 RPM. In this case, the IM works without any faults. As can be observed, there is no fault characteristic frequency in the Fourier transform (Fig. 5b and c).

The stator current signal has been shown in the steady-state mode for 12 seconds (Fig. 6a). The slip for this test is considered to be approximately 0.04. The fundamental frequency is dominant in the main signal of the stator current, and fault detection is challenged due to significant leakage effects (Fig. 6b). After implementing the proposed method on the stator current signal, the stator current signal is demodulated, and the TOEO signal is obtained (Fig. 6c). Finally, by using FFT, the fault characteristic frequency can be observed well in steady-state condition, (Fig. 6d).

The proposed method has also been tested on WRIM under light load conditions (Fig. 7). In this case, the rotational speed is 1460 rpm. As depicted in Fig. 7, by the proposed technique, the asymmetric fault has been also detected under low load conditions.

Such as asymmetry fault with adding external resistor is not a common fault condition in IMs, the proposed method has been tested on SCIM under BRB conditions. The rotor speed equal to 1430 RPM for 2BRBs.

Another test has been carried out for 3BRBs with 1410 RPM. According to Fig.8 and Fig.9, it can be observed that the presented method is able to detect asymmetric fault in any type of IM.

The Quantitative analysis of fault index in the presence of rotor asymmetric fault for SCIM and WRIM in full load condition is given in Table 3.

### C. TRANSIENT CONDITION

Here, we validate the effectiveness of the proposed approach in transient conditions on a WRIM. In this paper, the starting mode of the motor is not used to perform the test in transient mode. The starting mode causes a significant slip in the machine and makes the fault detection operation

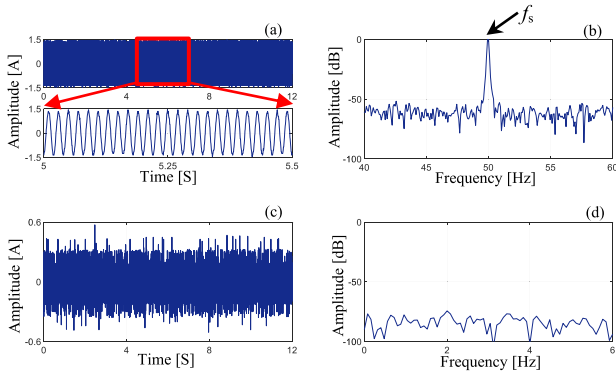


**FIGURE 5.** Steady state mode: healthy stator current signature of WRIM in a) time and b) frequency domains. Corresponding TOEO representations in c) time and d) frequency domains.

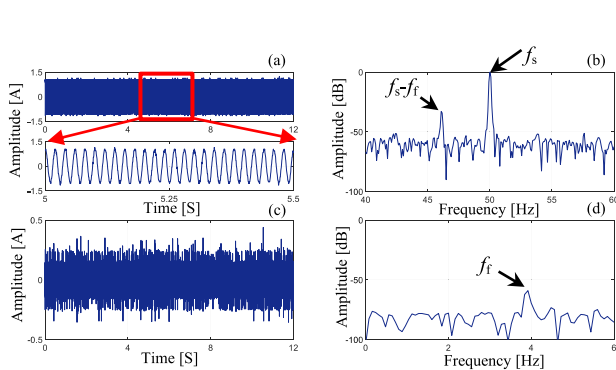


**FIGURE 6.** Steady-state mode: a) stator current signature of fault on WRIM with asymmetric fault in a) time and b) frequency domains. The corresponding TOEO signal in c) time and d) frequency domains.

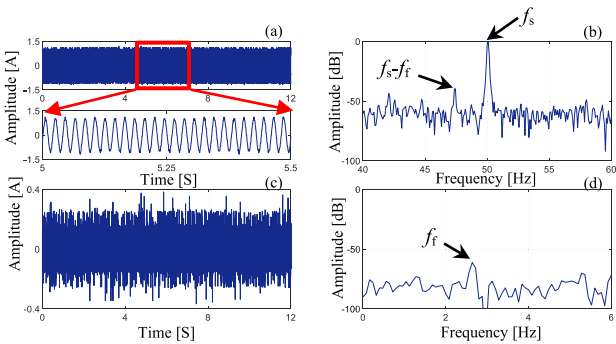


**FIGURE 7.** Steady-state mode of faulty WRIM under light load. a) Stator current signal in a) time and b) frequency domains. The corresponding TOEO signals in c) time and d) frequency domains.

straightforward in inverter-fed IMs. In small IMs the duration of transient condition is short (less than 400 ms). Therefore, high sampling frequency need to be used to collect the data. The proposed method has been tested during motor operation and small rotational speed changes to have a different challenge in transient mode.

The motor speed variations in two different modes, i.e., acceleration and deceleration are provided in Fig. 10a and Fig. 10b, respectively. The stator current signals were also

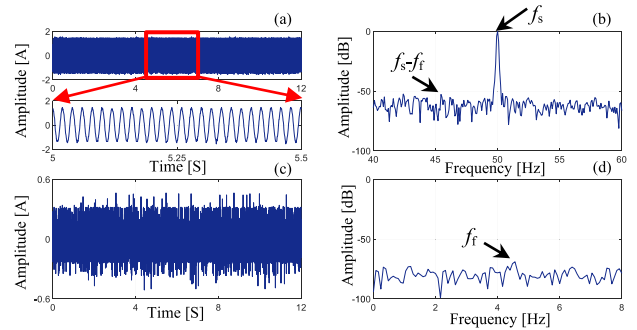


**FIGURE 8.** Steady-state mode of faulty SCIM with 2 BRBs. Stator current signal in a) time and b) frequency domains. The corresponding TOEO signals in c) time and d) frequency domains.

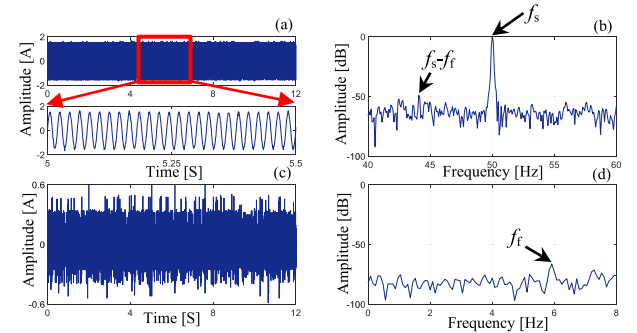


**FIGURE 9.** Steady-state mode of faulty SCIM with 3 BRBs. Stator current signal in a) time and b) frequency domains. The corresponding TOEO signals in a) time and b) frequency domains.

**TABLE 3.** Quantitative analysis of fault index in the presence of rotor asymmetric fault for SCIM and WRIM in full load condition.

SCIM	Value	WRIM	Value
Healthy	-83dB	Healthy	-74dB
1 BRB	-79dB	0.029 P.u.	-70dB
2 BRB	-70dB	0.059 P.u.	-61dB
3 BRB	-66dB	0.088 P.u.	-58dB

extracted in these two modes for 12 seconds and with a sampling frequency of 2.5 kHz (Fig. 10c and Fig. 10d).

Directly performing TF methods in the transient mode would fail the fault detection due to the leakage effects. Therefore, a necessary step involves the demodulation of the current signal. This demodulation process, as illustrated in Fig. 10e and Fig. 10f, plays a pivotal role in detecting asymmetric faults with high precision. Once the (TOEO) signal is obtained for each transient condition, the subsequent utilization of the MSST approach becomes instrumental in observing frequency variations over time, as depicted in Fig. 11. As previously mentioned, when applying MSST directly to the main signal, the fault characteristic frequency lacks clear traceability, as evidenced in Fig. 10a and Fig. 11b. However, a transformative outcome is achieved by demodulating the current signal using the proposed method, where the fault characteristic frequency becomes distinctly identifiable,

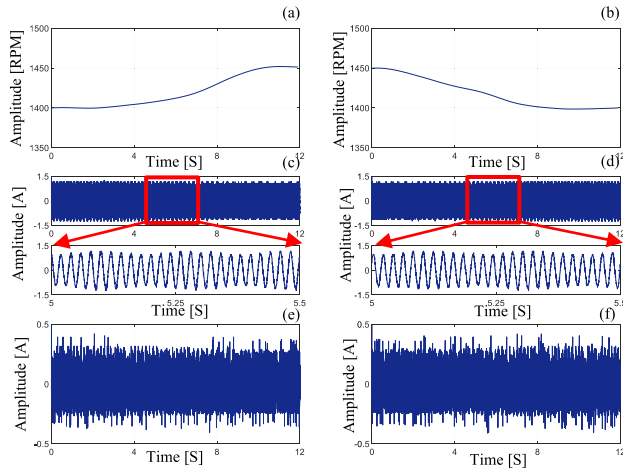


**FIGURE 10.** Transient mode on a WRIM: velocity variations in a) positive acceleration and b) deceleration modes. The stator current signal with asymmetric fault in c) acceleration and d) deceleration modes. Illustration of corresponding TOEO signal for e) acceleration and f) deceleration modes in time domain.

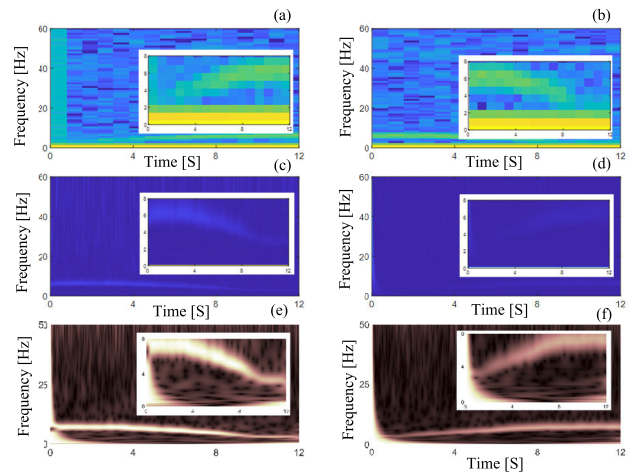


**FIGURE 12.** Transient mode on WRIM: comparative results with different frequency-based techniques. STFT on the TOEO signal in a) acceleration and b) deceleration modes. S-Transform of TOEO signal in c) deceleration and d) acceleration modes. CWT approach on TOEO signal in e) deceleration and f) acceleration modes.

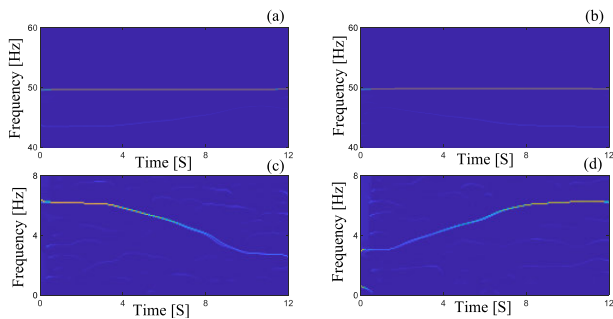


**FIGURE 11.** Transient mode on a WRIM: MSST of current signature in a) acceleration and b) deceleration conditions. Proposed MSST for TOEO signal under c) deceleration and d) acceleration conditions.

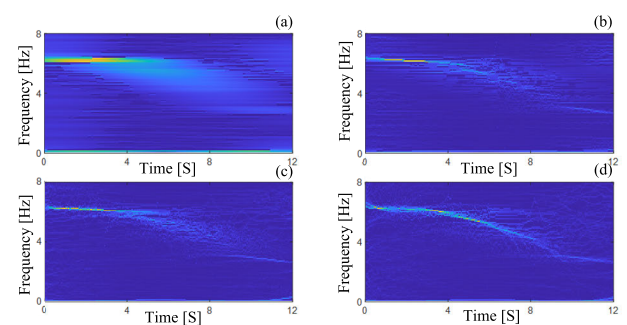


**FIGURE 13.** Transient mode on a WRIM: a) first order SST on TOEO signal in acceleration mode. b) Second order SST on TOEO signal in acceleration mode. c) Third order SST on TOEO signal in acceleration mode. d) Fourth order SST on TOEO signal in acceleration mode.

as exemplified in Fig. 11c and Fig. 11d. This methodological refinement enhances the accuracy and effectiveness of fault detection in transient conditions.

**VI. COMPARISON WITH PREVIOUS METHOD**

Within this section, we undertake a comparison between the proposed method and alternative time-frequency techniques such as the Stockwell transform (S-Transform), STFT and continuous wavelet transform (CWT), to affirm the efficacy of MSST. The comparison between Fig. 11 and Fig. 12 reveals that the proposed method outperforms other methods by generating a very narrow band with a high-resolution output response. Unlike STFT and other methods in Fig. 12, MSST is capable of detecting fault indices with a superior level of precision. Fig. 12 shows that CWT performs better than STFT and S-Transform, but still generates a very thick band not as accurate as our proposed method in Fig. 11.

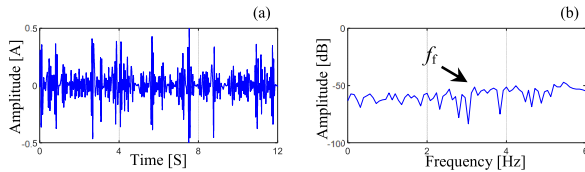
To better understand the effectiveness of the proposed method in the transient conditions, we have compared the detection results in four SST levels. As can be observed in

Fig.13, by increasing the order of SST the resolution of the output is improved. On the other hand, increasing the order of SST leads to an increase in the computational cost, so that we need 11 STFT to calculate fourth-order SST, while only one STFT is enough to calculate MSST.

The final comparison is devoted to assessing the demodulation quality. This comparison has been made between the proposed method and the EMD method. After implementing the EMD method, 10 IMFs are obtained, and the fifth IMF is used for fault detection. This IMF is the best IMF for fault detection compared to other IMFs. As it can be seen, fault detection by EMD method is not as good as the presented technique (Figure 14).

Considering the iterative nature of the MSST method, stopping the algorithm’s repetition presents a challenge which should be explored in the future. This could be done through adopting suitable criteria for termination of the algorithm. Also, further research is required to explore higher-order MSST to achieve enhanced resolution in the time-frequency





**FIGURE 14.** Empirical mode decomposition results for experimental data. a) 5<sup>th</sup> IMF obtained from EMD technique. b) FFT of 5<sup>th</sup> IMF.

plane output. Furthermore, there is a need to investigate a demodulation method characterized by low computational requirements and high separation power. In TOEO, the adverse effects of estimating higher-order derivatives of a discrete-time signal have not been explored in this work which could be examined in the future. It is crucial to investigate ways to effectively reduce high-frequency noise in derivative estimation to enable accurate induction motor fault detection.

## VII. CONCLUSION

This research introduces a new approach to isolating the characteristic frequency of asymmetric fault by a stator current phase in two stable and transient states. The TOEO strategy is proposed to demodulate the stator current signal. The presented method can significantly reduce the adverse effects of the spectral leakage of the fundamental frequency component. The presented method can effectively isolate and demodulate the stator current signal. In addition, the MSST technique is also presented for detection in the transient conditions. As a result, the presented method with low mathematical equations and high demodulation power can speed up the asymmetric fault detection process in IMs. As the future work, we plan to investigate how classification of various faults of the induction machines can be designed and applied to the output of our proposed method in this paper.

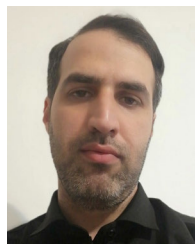
## REFERENCES

- [1] H. Wang, W. Sun, W. Sun, Y. Ren, Y. Zhou, Q. Qian, and A. Kumar, "A novel tool condition monitoring based on gramian angular field and comparative learning," *Int. J. Hydromechatronics*, vol. 6, no. 2, pp. 93–107, 2023, doi: [10.1504/ijhm.2023.130510](https://doi.org/10.1504/ijhm.2023.130510).
- [2] M. Ragnoli, M. Pavone, N. Epicoco, G. Pola, E. De Santis, G. Barile, and V. Stornelli, "A condition and fault prevention monitoring system for industrial computer numerical control machinery," *IEEE Access*, vol. 12, pp. 20919–20930, 2024, doi: [10.1109/ACCESS.2024.3359424](https://doi.org/10.1109/ACCESS.2024.3359424).
- [3] M. H. Marzabali, S. H. Kia, H. Henao, G.-A. Capolino, and J. Faiz, "Planetary gearbox torsional vibration effects on wound-rotor induction generator electrical signatures," *IEEE Trans. Ind. Appl.*, vol. 52, no. 6, pp. 4770–4780, Nov. 2016.
- [4] M. H. Marzabali, J. Faiz, G.-A. Capolino, S. H. Kia, and H. Henao, "Planetary gear fault detection based on mechanical torque and stator current signatures of a wound rotor induction generator," *IEEE Trans. Energy Convers.*, vol. 33, no. 3, pp. 1072–1085, Sep. 2018.
- [5] A. Choudhary, D. Goyal, S. L. Shimi, and A. Akula, "Condition monitoring and fault diagnosis of induction motors: A review," *Arch. Comput. Methods Eng.*, vol. 26, no. 4, pp. 1221–1238, Sep. 2019, doi: [10.1007/s11831-018-9286-z](https://doi.org/10.1007/s11831-018-9286-z).
- [6] S. M. K. Zaman, X. Liang, and W. Li, "Fault diagnosis for variable frequency drive-fed induction motors using wavelet packet decomposition and greedy-gradient max-cut learning," *IEEE Access*, vol. 9, pp. 65490–65502, 2021.
- [7] M. E. E. Atta, D. K. Ibrahim, and M. I. Gilany, "Broken bar fault detection and diagnosis techniques for induction motors and drives: State of the art," *IEEE Access*, vol. 10, pp. 88504–88526, 2022, doi: [10.1109/ACCESS.2022.3200058](https://doi.org/10.1109/ACCESS.2022.3200058).
- [8] K. Yatsugi, S. E. Pandarakone, Y. Mizuno, and H. Nakamura, "Common diagnosis approach to three-class induction motor faults using stator current feature and support vector machine," *IEEE Access*, vol. 11, pp. 24945–24952, 2023, doi: [10.1109/ACCESS.2023.3254914](https://doi.org/10.1109/ACCESS.2023.3254914).
- [9] M. H. Marzabali, R. Bazghandi, and V. Abolghasemi, "Rotor asymmetries faults detection in induction machines under the impacts of low-frequency load torque oscillation," *IEEE Trans. Instrum. Meas.*, vol. 71, pp. 1–11, 2022, doi: [10.1109/TIM.2022.3201950](https://doi.org/10.1109/TIM.2022.3201950).
- [10] S. H. Kia, A. E. Hajjaji, and M. H. Marzabali, "Planetary gear tooth fault detection using stator current space vector analysis in induction machine-based systems," in *Proc. 23rd Int. Conf. Mechatronics Technol. (ICMT)*, Oct. 2019, pp. 1–6, doi: [10.1109/ICMECT.2019.8932157](https://doi.org/10.1109/ICMECT.2019.8932157).
- [11] P. Xia, Y. Huang, Z. Tao, C. Liu, and J. Liu, "A digital twin-enhanced semi-supervised framework for motor fault diagnosis based on phase-contrastive current dot pattern," *Rel. Eng. Syst. Saf.*, vol. 235, Jul. 2023, Art. no. 109256.
- [12] V. Gurusamy, K. H. Baruti, M. Zafarani, W. Lee, and B. Akin, "Effect of magnets asymmetry on stray magnetic flux based bearing damage detection in PMSM," *IEEE Access*, vol. 9, pp. 68849–68860, 2021, doi: [10.1109/ACCESS.2021.3076779](https://doi.org/10.1109/ACCESS.2021.3076779).
- [13] J. A. Ramirez-Nunez, J. A. Antonino-Daviu, V. Climente-Alarcón, A. Quijano-López, H. Razik, R. A. Osornio-Rios, and R. D. J. Romero-Troncoso, "Evaluation of the detectability of electromechanical faults in induction motors via transient analysis of the stray flux," *IEEE Trans. Ind. Appl.*, vol. 54, no. 5, pp. 4324–4332, Sep. 2018, doi: [10.1109/TIA.2018.2843371](https://doi.org/10.1109/TIA.2018.2843371).
- [14] Y. Zhou, H. Wang, G. Wang, A. Kumar, W. Sun, and J. Xiang, "Semi-supervised multiscale permutation entropy-enhanced contrastive learning for fault diagnosis of rotating machinery," *IEEE Trans. Instrum. Meas.*, vol. 72, pp. 1–10, 2023.
- [15] Z. Liu, X. Wang, and L. Zhang, "Fault diagnosis of industrial wind turbine blade bearing using acoustic emission analysis," *IEEE Trans. Instrum. Meas.*, vol. 69, no. 9, pp. 6630–6639, Sep. 2020, doi: [10.1109/TIM.2020.2969062](https://doi.org/10.1109/TIM.2020.2969062).
- [16] B. A. Vinayak, K. A. Anand, and G. Jagadanand, "Wavelet-based real-time stator fault detection of inverter-fed induction motor," *IET Electric Power Appl.*, vol. 14, no. 1, pp. 82–90, Jan. 2020.
- [17] W. Li, Z. Zhang, F. Auger, and X. Zhu, "Theoretical analysis of time-reassigned synchrosqueezing wavelet transform," *Appl. Math. Lett.*, vol. 132, Oct. 2022, Art. no. 108141.
- [18] Z.-I. Huang, J. Zhang, T.-H. Zhao, and Y. Sun, "Synchrosqueezing S-transform and its application in seismic spectral decomposition," *IEEE Trans. Geosci. Remote Sens.*, vol. 54, no. 2, pp. 817–825, Feb. 2016.
- [19] L. Ke, Y. Zhang, B. Yang, Z. Luo, and Z. Liu, "Fault diagnosis with synchrosqueezing transform and optimized deep convolutional neural network: An application in modular multilevel converters," *Neurocomputing*, vol. 430, pp. 24–33, Mar. 2021.
- [20] Q. Wang, Y. Li, S. Chen, and B. Tang, "Matching demodulation synchrosqueezing S transform and its application in seismic time-frequency analysis," *IEEE Geosci. Remote Sens. Lett.*, vol. 19, 2022, Art. no. 7501505, doi: [10.1109/LGRS.2020.3047892](https://doi.org/10.1109/LGRS.2020.3047892).
- [21] Z. Huang, D. Wei, Z. Huang, H. Mao, X. Li, R. Huang, and P. Xu, "Parameterized local maximum synchrosqueezing transform and its application in engineering vibration signal processing," *IEEE Access*, vol. 9, pp. 7732–7742, 2021, doi: [10.1109/ACCESS.2020.3031091](https://doi.org/10.1109/ACCESS.2020.3031091).
- [22] D.-H. Pham and S. Meignen, "High-order synchrosqueezing transform for multicomponent signals analysis—With an application to gravitational-wave signal," *IEEE Trans. Signal Process.*, vol. 65, no. 12, pp. 3168–3178, Jun. 2017.
- [23] Y. Hu, X. Tu, F. Li, and G. Meng, "Joint high-order synchrosqueezing transform and multi-taper empirical wavelet transform for fault diagnosis of wind turbine planetary gearbox under nonstationary conditions," *Sensors*, vol. 18, no. 1, p. 150, Jan. 2018.
- [24] M. Singh and A. G. Shaik, "Faulty bearing detection, classification and location in a three-phase induction motor based on stockwell transform and support vector machine," *Measurement*, vol. 131, pp. 524–533, Jan. 2019.
- [25] G. Yu, Z. Wang, and P. Zhao, "Multisynchrosqueezing transform," *IEEE Trans. Ind. Electron.*, vol. 66, no. 7, pp. 5441–5455, Jul. 2019, doi: [10.1109/TIE.2018.2868296](https://doi.org/10.1109/TIE.2018.2868296).

- [26] F. Auger and P. Flandrin, "Improving the readability of time-frequency and time-scale representations by the reassignment method," *IEEE Trans. Signal Process.*, vol. 43, no. 5, pp. 1068–1089, May 1995.
- [27] G. Thakur and H.-T. Wu, "Synchrosqueezing-based recovery of instantaneous frequency from nonuniform samples," *SIAM J. Math. Anal.*, vol. 43, no. 5, pp. 2078–2095, Jan. 2011.
- [28] P. Maragos and A. Potamianos, "Higher order differential energy operators," *IEEE Signal Process. Lett.*, vol. 2, no. 8, pp. 152–154, Aug. 1995, doi: [10.1109/97.404130](https://doi.org/10.1109/97.404130).
- [29] R. Bazghandi, M. H. Marzebali, and V. Abolghasemi, "Asymmetrical fault detection in induction motors through elimination of load torque oscillations effects in the slight speed variations and steady-state conditions," *IEEE J. Emerg. Sel. Topics Ind. Electron.*, vol. 4, no. 3, pp. 725–733, Jul. 2023, doi: [10.1109/JESTIE.2022.3204485](https://doi.org/10.1109/JESTIE.2022.3204485).
- [30] T. A. Garcia-Calva, D. Morinigo-Sotelo, A. Garcia-Perez, D. Camarena-Martinez, and R. D. J. Romero-Troncoso, "Demodulation technique for broken rotor bar detection in inverter-fed induction motor under non-stationary conditions," *IEEE Trans. Energy Convers.*, vol. 34, no. 3, pp. 1496–1503, Sep. 2019.
- [31] W. Wang, X. Song, G. Liu, Q. Chen, W. Zhao, and H. Zhu, "Induction motor broken rotor bar fault diagnosis based on third-order energy operator demodulated current signal," *IEEE Trans. Energy Convers.*, vol. 37, no. 2, pp. 1052–1059, Jun. 2022, doi: [10.1109/TEC.2021.3121788](https://doi.org/10.1109/TEC.2021.3121788).
- [32] R. Pucho-Panadero, J. Martinez-Roman, A. Sapena-Bano, and J. Burriel-Valencia, "Diagnosis of rotor asymmetries faults in induction machines using the rectified stator current," *IEEE Trans. Energy Convers.*, vol. 35, no. 1, pp. 213–221, Mar. 2020, doi: [10.1109/TEC.2019.2951008](https://doi.org/10.1109/TEC.2019.2951008).
- [33] R. Ziani, A. Hammami, F. Chaari, A. Felkaoui, and M. Haddar, "Gear fault diagnosis under non-stationary operating mode based on EMD, TKEO, and shock detector," *Comp. Rendus. Mécanique*, vol. 347, no. 9, pp. 663–675, Sep. 2019.
- [34] Y. Yang, Z. K. Peng, X. J. Dong, W. M. Zhang, and G. Meng, "General parameterized time-frequency transform," *IEEE Trans. Signal Process.*, vol. 62, no. 11, pp. 2751–2764, Jun. 2014, doi: [10.1109/TSP.2014.2314061](https://doi.org/10.1109/TSP.2014.2314061).
- [35] S. Wang, X. Chen, G. Cai, B. Chen, X. Li, and Z. He, "Matching demodulation transform and synchrosqueezing in time-frequency analysis," *IEEE Trans. Signal Process.*, vol. 62, no. 1, pp. 69–84, Jan. 1, 2014, doi: [10.1109/TSP.2013.2276393](https://doi.org/10.1109/TSP.2013.2276393).
- [36] T. Oberlin, S. Meignen, and V. Perrier, "Second-order synchrosqueezing transform or invertible reassignment? Towards ideal time-frequency representations," *IEEE Trans. Signal Process.*, vol. 63, no. 5, pp. 1335–1344, Mar. 2015, doi: [10.1109/TSP.2015.2391077](https://doi.org/10.1109/TSP.2015.2391077).
- [37] V. Fernandez-Cavero, D. Morinigo-Sotelo, O. Duque-Perez, and J. Pons-Llinares, "A comparison of techniques for fault detection in inverter-fed induction motors in transient regime," *IEEE Access*, vol. 5, pp. 8048–8063, 2017, doi: [10.1109/ACCESS.2017.2702643](https://doi.org/10.1109/ACCESS.2017.2702643).



**REZA BAZGHANDI** received the B.Sc. degree in electrical engineering from Islamic Azad University, West Tehran Branch, Tehran, Iran, in 2020, and the M.Sc. degree in electrical power engineering from Shahrood University of Technology, Shahrood, Iran. His main research interests include fault diagnose in electrical machine.



**MOHAMMAD HOSEINTABAR MARZEBALI** received the B.Sc. degree in electrical power engineering from the University of Mazandaran, Mazandaran, Iran, in 2007, and the M.Sc. degree in electrical power engineering from Shiraz University of Technology, Shiraz, Iran, in 2010. Since 2014, he has been an Associate Professor with Shahrood University of Technology, Shahrood, Iran. His research interests include fault diagnose in electrical machine and modular multilevel converters.



**VAHID ABOLGHASEMI** (Senior Member, IEEE) received the Ph.D. degree in signal processing from the University of Surrey, Guildford, U.K., in 2011. He is currently an Associate Professor with the School of Computer Science and Electronic Engineering, University of Essex, Colchester, U.K. His main research interests include signal and image processing, compressive sensing, and machine learning. His expertise extends to cutting-edge technologies, including smart and adaptive low-power sensing and communication, wireless image transmission, compressed and lightweight neural networks, and artificial intelligence.

...